Int J Clin Exp Pathol 2015;8(2):1451-1458
www.ijcep.com /ISSN:1936-2625/IJCEP0004796

Original Article

MiRNA profile of osteosarcoma with CD117 and stro-1 expression: miR-1247 functions as an onco-miRNA by targeting MAP3K9

Fuyou Zhao[1*], Jie Lv[2*], Huaiyong Gan[3*], Yumei Li[1], Ri Wang[1], Haoran Zhang[1], Qiong Wu[1], Yuqing Chen[4]

Departments of [1]Medical Oncology, [3]Pathology, [4]Respiratory Diseases, The First Affiliated Hospital of Bengbu Medical College, Bengbu, Anhui 233000, China; [2]Department of Microbiology, Bengbu Medical College, Bengbu, Anhui 233000, China. [*]Equal contributors.

Received December 13, 2014; Accepted February 5, 2015; Epub February 1, 2015; Published February 15, 2015

Abstract: microRNAs (miRNA) are regulators of gene expression, but little is known about miRNA expression profiles in stem cells of osteosarcoma (OS). C117 and Stro-1 are known stem cell markers of OS. In the study, CD117 and stro-1 positive ($CD117^+stro\text{-}1^+$) and CD117 and stro-1 negative ($CD117^-stro\text{-}1^-$) cells were isolated from MG63 cells $CD117^+stro\text{-}1^+$ cells showed more metastatic ability and stem cell formation rate than $CD117^-stro\text{-}1^-$ ones. To find the difference between $CD117^+stro\text{-}1^+$ and $CD117^-stro\text{-}1^-$ cells, the miRNA expression profile was examined using DNA microarray. MicroRNAs were differentially expressed in osteosarcoma cells with $CD117^+stro\text{-}1^+$ and $CD117^-stro\text{-}1^-$. The significant miRNAs included miR-15a, miR-302a, miR-423-5p, miR-1247, miR-1243 and others, which were confirmed by real time RT-PCR. The significant down-regulated miR-1247 was confirmed that was a potential tumor suppressor by targeting MAP3K9. Our results indicated that dysregulation of miRNAs is involved in osteosarcoma and miR-1247 plays an important role in progression of osteosarcoma.

Keywords: miR-1247, miRNA profile, osteosarcoma, MAP3K9

Introduction

Osteosarcoma is the most common malignant bone tumor in adolescent. Initially, many patients with osteosarcoma respond to chemotherapy, but those which are metastatic have extremely low survival rates [1]. The 5-year survival rate in patients without metastasis at diagnosis is about 60-70% and the clinical outcomes in patients with metastasis are very worse [2, 3]. However, the mechanisms in osteosarcoma initiation and progression are not clear.

Cancer stem cells (CSCs) have been identified in many types of cancers, such as leukemia, breast tumor, brain tumor, prostate tumor and melanoma and other types of cancer [4-7]. CSCs are identified mainly based on detection of molecule markers, intrinsic cellular properties and functional characterization [4]. There are multiple markers have been employed to identify CSCs of osteosarcoma, such as CD133 [6], CD117/Stro-1 [7]. CSCs with these marks shared similar stem-like properties, such as self-renewal, differentiation, drug resistance, tumorigenicity and multi-potency.

MicroRNAs (miRNAs) are small non-coding RNA molecules with 18-25 nucleotides in length. Through completely or partially complementary with the 3'-untranslated region (3'UTR) of specific messenger RNAs, miRNAs induce various target genes, silencing and participating in various cell biological processes [8-10]. Moreover, miRNAs were demonstrated to play critical roles in the development and progression of cancers and have been found to have positive or negative effects on cell proliferation, apoptosis, and invasion in various cancer cells. Recently, numerous studies reported the association between dysregulation of miRNAs and OS, switching from profiling studies to biological demonstrations of the causal role of these small molecules in OS pathogenesis, and the possible implications as biomarkers or therapeutic tools [11, 12]. However, there needs research to better understanding miRNAs in OS stem cells.

In this study, we explored miRNA expression profile of $CD117^{+}Stor\text{-}1^{+}$ cells and selected the significant miR-1247. Further, the significant miRNAs were verified by TaqMan RT-PCR analysis. Subsequently, we completed a series of cellular function experiments to investigate the role of miR-1247 in osteosarcoma. Since the involvement of miR-1247 in osteosarcoma carcinogenesis is largely unexplored, we have investigated osteosarcoma cell lines underexpressing miR-1247, with the aim to study its effects on cellular progressions and to identify the mechanisms involved. In addition, we found that MAP3K9 was a target gene of miR-1247 and MAP3K9 could promote OS proliferation and sphere formation.

Materials and methods

Patients and tissue specimens

Formalin fixed paraffin-embedded specimens of osteosarcoma tissues were collected from the First Affiliated Hospital Of Bengbu Medical College (Anhui, China). The matched normal tissues were obtained 5 cm distant from the tumor margin, which were further confirmed by pathologists. All patients did not undergo any therapy before recruitment to this research. Use of the tissue samples for all experiments was approved by Ethics Committee of the instruction.

Cell lines and cell culture

Human osteosarcoma cell lines (HOS, Saos-2, U2OS and MG-63) or normal osteoblast cells (NHOst) were obtained from the American Type Culture Collection (ATCC, Manassas, VA, USA). HEK293T cells were stored at our lab. The cells were maintained in Dulbecco's modified Eagle medium (DMEM, Gibco, Life Technologies, Darmstadt, Germany), supplemented with 10% fetal bovine serum (FBS; PAA, Pasching, Austria) and streptomycin (100 μg/mL), penicillin (100 U/mL). Cultures were incubated in a humidified atmosphere of 5% CO_2 at 37°C.

Fluorescence-activated cell sorting (FACS)

Total 10^4 cells were suspended in FACS buffer (PBS with 0.1% BSA and 0.1% Triton X100) followed by incubation with FITC conjugated anti-CD117 for 15 min at room temperature. Cells were then washed with PBS and re-suspended in PBS for FACS analysis.

miRNA precursor expression profiling

Total RNA was isolated from the cell lines or tissues in 1 ml of Trizol (Invitrogen, USA). RNA concentration was determined by analyzing 1 μl of solution using the ND-1000 micro-spectrophotometer (NanoDrop Technologies, Wilmington, DE). RNA integrity was evaluated using the Agilent 2100 Bioanalyzer (Agilent Technologies, Palo Alto, CA). RNA with a RIN ≥ 4 was included in the study. RNA was briefly treated with RNase-free DNAase I and cDNA was synthesized from 1 μg of total RNA using gene specific primers to 222 miRNA precursors plus 18S rRNA. The expression of 222 miRNA precursors was profiled using a real-time quantitative PCR assay. Duplicate PCRs were performed for each miRNA precursor gene in each sample of cDNA. The mean *C*T was determined from the duplicate PCRs. Relative gene expression was calculated as 2-(*C*TmiRNA-*C*T18S rRNA).

RNA isolation and real-time RT-PCR

Total RNA, following the manufacturer's instructions, was isolated from the cells using Trizol reagent (Invitrogen, Carlsbad, CA, USA). Briefly, the cells were lysed in TRIzol and then mixed with chloroform. The lysate was centrifuged to separate RNA, DNA and protein, total RNA recovered, precipitated with isopropanol, washed in 75% ethanol to remove impurities before dissolved in water. After that, 2 μg of RNA was taken and treated with DNase to remove contaminating DNA prior to the reverse transcription to cDNA using SYBR® PCR Kit (Takara, Japan). To measure mRNA expression, real-time RT-PCR was performed using a sequence detector (ABI-Prism, Carlsbad, CA, USA). Primers were purchased from Invitrogen. The relative expression levels were calculated by comparing Ct values of the samples with those of the reference, all data normalized to the internal control GAPDH.

Tumor spheroid assay

Spheroid forming assays were performed as described. In brief, cells were plated in six-well ultralow attachment plates (Corning Inc., Corning, NY, USA) at a density of 1,000 cells/ml in DMEM supplemented with 1% N2 Supplement (Invitrogen, Carlsbad, CA, USA), 2% B27 Supplement (Invitrogen, Carlsbad, CA, USA), 20 ng/ml human platelet growth factor (Sigma-Aldrich, Saint Louis, MO, USA), 100 ng/ml epi-

dermal growth factor (Invitrogen, Carlsbad, CA, USA) and 1% antibiotic-antimycotic (Invitrogen) at 37°C in a humidified atmosphere of 5% CO_2. Spheroid were collected after 7 days and dissociated with Accutase (Innovative Cell Technologies, Inc.). The cells obtained from dissociation were sieved through a 40-μm filter, and counted by coulter counter using trypan blue dye.

MTT assay

MTT assay was employed to detect the growth of glioma cells and the growth curve was delineated. Logarithmic phase cells were collected, and the concentration of the cell suspension was adjusted to 5000 cells per well (The edge wells of the plate are filled with aseptic PBS buffer). The cells were incubated at 37°C, 5% CO_2 until cells cover the bottom of the well (a flat-bottom 96-well plate), and then the cells were cultured. 20 μl of the MTT solution was added to each well (5 mg/ml, 0.5% MTT) and the cells were continued to culture for 4 h. After the incubation, the supernatant was discarded and 150 μl dimethyl sulfoxide was added to each well, and the culture plate was shaked at low speed for 10 min until crystal dissolved completely. The ELISA reader was used to measure the absorbance at 570 nm.

Colony forming assay

Cells in logarithmic growth phase were digested in 0.5% trypsin/0.04% EDTA and single cell suspension was prepared. Then, these cells were added to 6-well plates (200 cells/well) followed by incubation at 37°C in an environment with saturated humidity and 5% CO_2 for 24 h. Non-adherent cells were removed. After culture for 10-14 days, lcolonies were present. These cells were seeded into 96-well plates followed by incubation at 37°C in an environment with saturated humidity and 5% CO_2. The colony forming efficiency and the morphology of colonies were observed. The size of colonies was measured and cells in each colony were counted. At this time, cells were divided into early passaging group and late passaging group. In the early passaging group, cells with target number were digested in 0.5% trypsin/0.04% EDTA for preparation of single cell suspension. These cells were then seeded into 96-well plates. In the late passaging group, cells were digested in 0.5% trypsin/0.04% EDTA for preparation of single cell suspension. These cells were then seeded into 96-well plates.

Cell cycle assay

Cells were harvested by trypsinization, washed in ice-cold PBS, fixed in ice-cold 80% ethanol in PBS, centrifuged at 4°C and resuspended in chilled PBS. Bovine pancreatic RNAase (Sigma-Aldrich) was added at a final concentration of 2 μg/ml, incubated at 37°C for 30 min, then 20 μg/ml propidium iodide (Sigma-Aldrich, Saint Louis, MO, USA) was added and incubated for 20 min at room temperature. In each group, 50,000 cells were analyzed by flow cytometry (FACSCalibur; BD Biosciences, San Jose, CA, USA).

Western blot analysis

Western blots were performed as we described elsewhere. In brief, cells were lysed in RIPA buffer containing 1 X protease inhibitor cocktail, and protein concentrations were determined using the Bradford assay (Bio-Rad, Philadelphia, PA, USA). Proteins were separated by 12.5% SDS/PAGE and transferred to membranes (Millipore, Bedford, MA, USA) at 55 V for 4 h at 4°C. After blocking in 5% nonfat dry milk in TBS, the membranes were incubated with primary antibodies at 1:1,000 dilution in TBS overnight at 4°C, washed three times with TBS-Tween 20, and then incubated with secondary antibodies conjugated with horseradish peroxidase at 1:5,000 dilution in TBS for 1 hour at room temperature. Membranes were washed again in TBS-Tween 20 for three times at room temperature. Protein bands were visualized on X-ray film using an enhanced chemiluminescence detection system.

Statistical analysis

Each experiment was repeated at least three times. Statistical analyses were performed using SPSS 15.0 (SPSS Inc.; Chicago, IL, USA). Data are presented as the mean 6 standard deviation. Statistical analyses were performed with either an analysis of variance (ANOVA) or Student's t-test, and the statistical significance level was set at a = 0.05 (two-side).

Results

Cells expressing CD117 and Stro-1 positive shows stem cell properties.

To compare with miRNA expression between the positive CD117 and Stro-1 OS cells

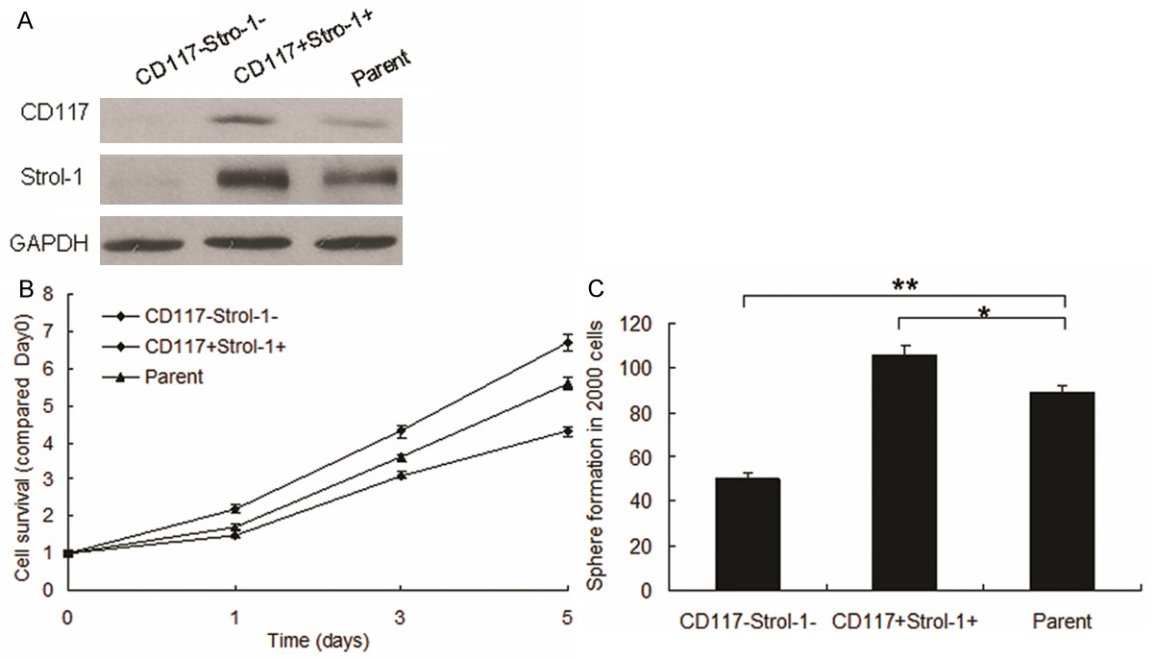

Figure 1. CD117$^+$ and Stro-1$^+$ promotes proliferation and stem-cell properties in cells. A. CD117 and Stro-1 expression were verified by Western blot. MG63 cells were cultured and CD117$^+$Stro-1$^+$ cells were sorted out by flow cytometry and total protein was collected for Western blot. B. MG63 Cells proliferation was analyzed by MTT assay. CD117$^+$Stro-1$^+$ cells and CD117$^-$Stro-1$^-$ cells were seeded in 96 well plate, added MTT in the day of 0, 1, 3, 5 and then recorded at the wavelength 570 nm. C. Stem cell sphere formation was performed in CD117$^+$Stro-1$^+$ cells and CD117$^-$Stro-1$^-$ cells. The cells were cultured in medium especially for stem cells and counted the spheres after 2 weeks. Experiments were repeated for at least three times. $^{**}P < 0.01$ compared with scramble group. $^{*}P < 0.05$ compared with scramble group.

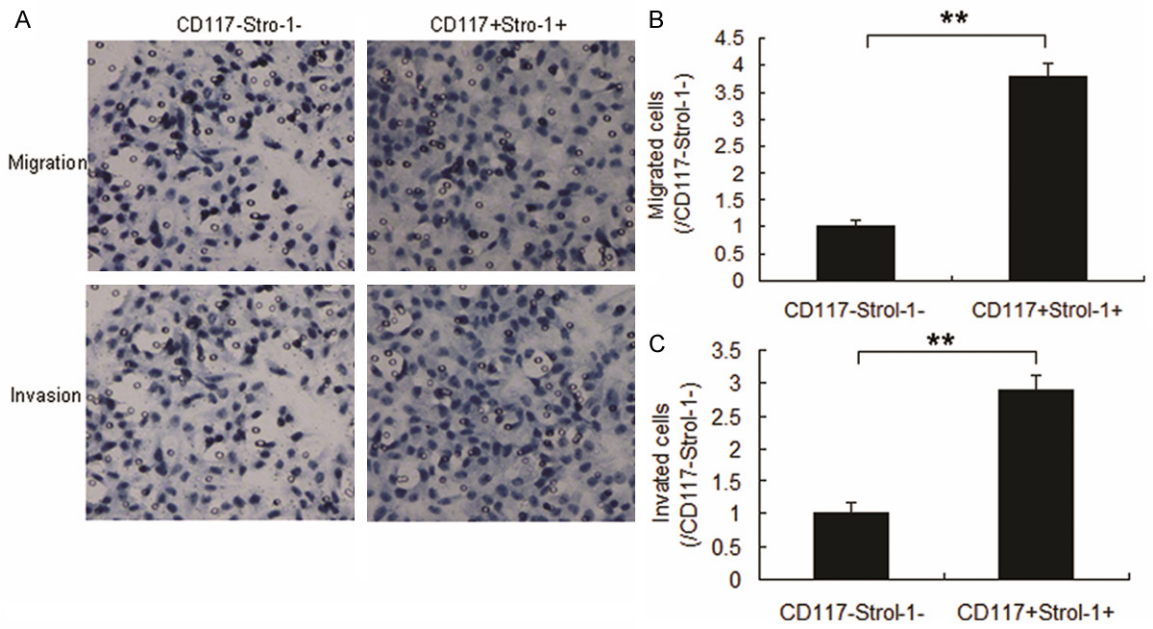

Figure 2. CD117$^+$Stro-1$^+$ cells efficiently initiate tumors with a high frequency of metastasis. (A) Migration and invasion of MG63 cells with CD117$^+$Stro-1$^+$ and CD117$^-$Stro-1$^-$. Cells (10^4) were seeded in the up-chamber and migrated cells were counted 24 hours later. The invasion assay different from migration was that there as Matrigel in the up-chamber. (B) Qualification of migrated cells from A. (C) Qualification of invaded cells from A. Experiments were

repeated for at least three times. **$P < 0.01$ compared with scramble group. *$P < 0.05$ compared with scramble group.

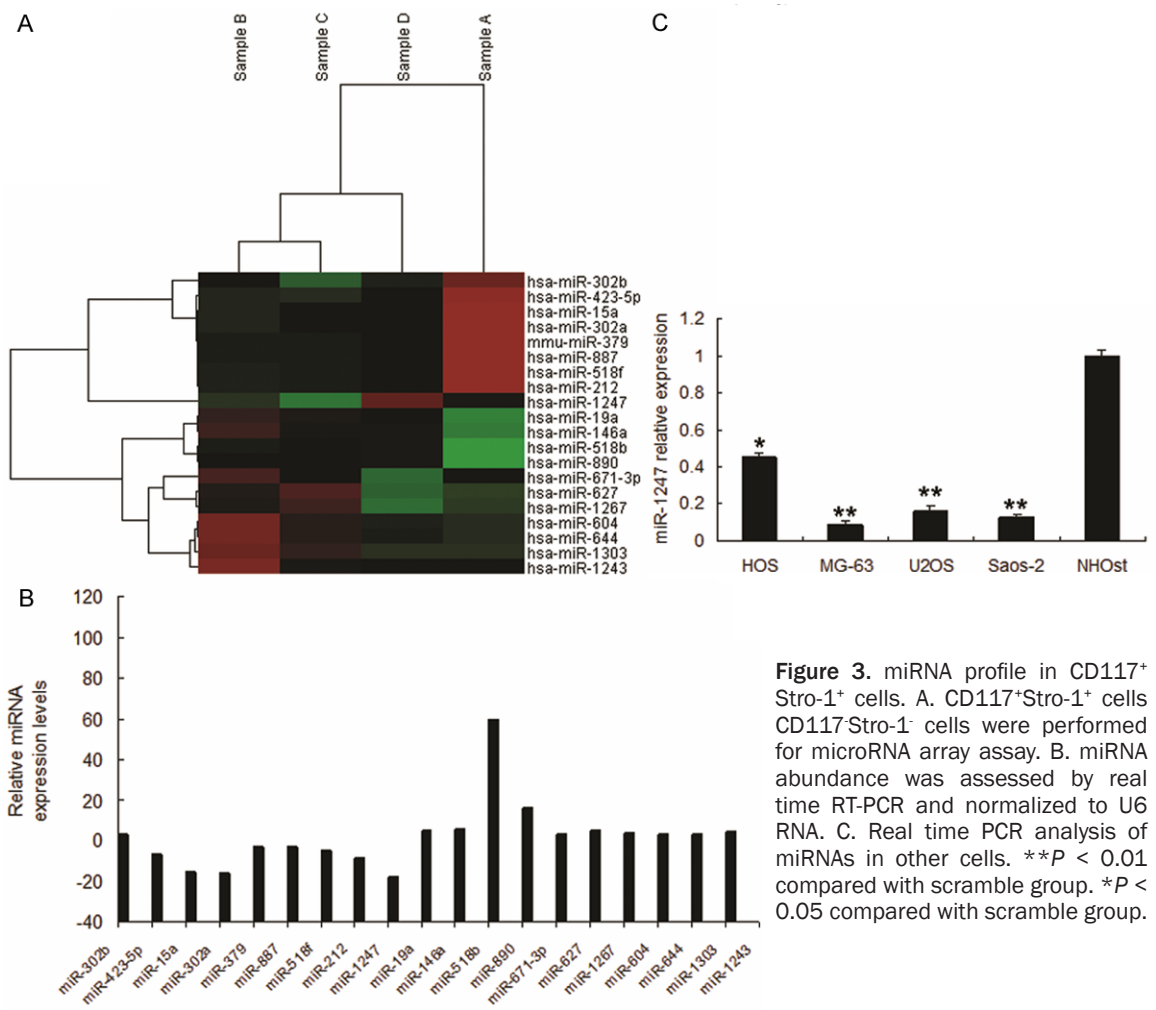

Figure 3. miRNA profile in CD117$^+$ Stro-1$^+$ cells. A. CD117$^+$Stro-1$^+$ cells CD117$^-$Stro-1$^-$ cells were performed for microRNA array assay. B. miRNA abundance was assessed by real time RT-PCR and normalized to U6 RNA. C. Real time PCR analysis of miRNAs in other cells. **$P < 0.01$ compared with scramble group. *$P < 0.05$ compared with scramble group.

(CD117$^+$Stro-1$^+$) and negative ones (CD117$^-$ Stro-1$^-$), CD117$^+$Stro-1$^+$ MG63 cells were sorted out using flow cytometry. The overexpressed genes were verified using Western Blot (**Figure 1A**). After cell separation and identification by flow cytometry, the cell proliferation and sphere formation were tested by MTT and sphere formation assays respectively and the results showed that CD117$^+$Stro-1$^+$ cells took more proliferation and sphere formation (**Figure 1B** and **1C**). These data indicated that CD117$^+$Stro-1$^+$ MG63 cells showed stem like cells.

CD117$^+$Stro-1$^+$ cells efficiently initiate tumors with a high frequency of metastasis

The most significant property of cancer stem cells is their ability to initiate tumors. Therefore, CD117$^+$Stro-1$^+$ cells were seeded in the up-chamber of transwell to analyze the metastatic ability. Compared with the CD117$^-$Stro-1$^-$ cells, positive ones showed higher migration (**Figure 2A**, **2B**) and invasion (**Figure 2A**, **2C**). These indicated that CD117 and Stro-1 could promote OS metastasis.

miRNA profile in CD117$^+$Stro-1$^+$ cells

To determine the miRNA expression pattern in CD117$^+$Stro-1$^+$ cells and CD117$^-$Stro-1$^-$ cells, the expression of 768 miRNAs was analyzed utilizing Affymetrix Gene Chips. Data demonstrated distinct expression patterns in the two groups, with differentially expressed miRNAs between the groups (**Figure 3A**). To further determine the miRNAs, we performed real time RT-PCR to

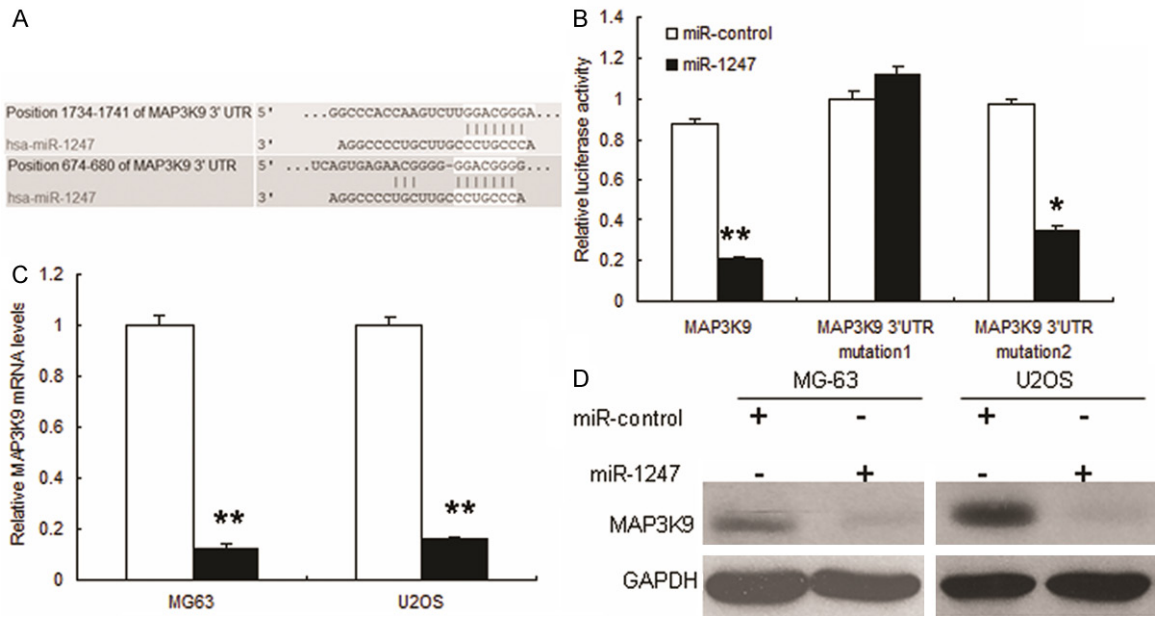

Figure 4. miR-1247 targets MAP3K9 in MG-63 cells. (A) Schematic representation of MAP3K9 3'UTR showing putative miRNA target sites. There exist putative binding sites in the 3'UTR of miR-1247. (B) Relative luciferase activity of the indicated MAP3K9 reporter construct in MG-63 cells, co-transfected with miR-1247 mimics or scramble mimics, is shown. In cells co-transfected with 3'-UTR vectors and miR-1247 mimic, the luciferase activity was suppressed relative to mutant construct groups; and (C, D) Quantitative RT-PCR and Western blot assays were performed to detect the expression of MAP3K9 upon transfection with miR-1247 mimics or scramble mimics. The expressions of mRNA and protein were suppressed upon transfection with miR-1247. $^{**}P < 0.01$ compared with scramble group. $^{*}P < 0.05$ compared with scramble group.

confirm the results (**Figure 3B**). Of the 20 miRNAs, we confirmed eight most significant miRNAs by qRT-PCR in the selected cells with $CD117^{+}$ and $Stro\text{-}1^{+}$. The down-regulated miRNAs included miR-15a, miR-302a, miR-423-5p, miR-212 and miR-1247 and up-regulated included miR-518b, miR-890 and miR-1243. Thus, we chosen the significant miR-1247 for further analysis. The data was verified in other OS cell lines (**Figure 3C**).

miR-1247 targets MAP3K9 in MG-63 cells

miRNAs regulate the expression of mRNAs by targeting the 3'UTR of relative mRNAs. To explore the mechanisms involved in miR-1247-mediated tumor suppression, putative targets of miR-1247 were searched using the prediction program and MAP3K9 was selected out due to its constitutive over-expression in OS. As shown in **Figure 4A**, there exists two putative binding sites of miR-1247 in the 3'UTR of MAP3K9.

To determine whether or not the three putative binding sites perform a function, we performed luciferase assays. The putative 3'UTR of MAP3K9 gene was amplified and cloned into a luciferase reporter vector, and the constructs with each binding sites mutated. These constructs were transiently transfected into MG-63 cells, and the transcription activities were measured using a dual-luciferase detection system. As expected, significant repression of luciferase activities were observed in MG-63 cells co-transfected with pGL3-MAP3K9 3'-UTR vector and miR-1247 mimic compared to mutant constructs groups. Each single mutant construct, exhibited a lower inhibitory effect on luciferase activity compared with the pGL3- 3'-UTR vector after miR-1247 co-transfection, showed complete reversal of inhibitor effect of miR-1247 co-transfection (**Figure 4B**), suggesting that miR-1247 suppressed the transcription activity of the MAP3K9 gene by targeting the 3'UTR. mRNA and protein levels of MAP3K9 were also down-regulated when the MG63 cells with miR-1247 overexpression (**Figure 4C** and **4D**).

MAP3K9 promotes OS proliferation and shows stem cells properties

To investigate role of MAP3K9 in OS progression, MG63 cells were infected with lentivirus

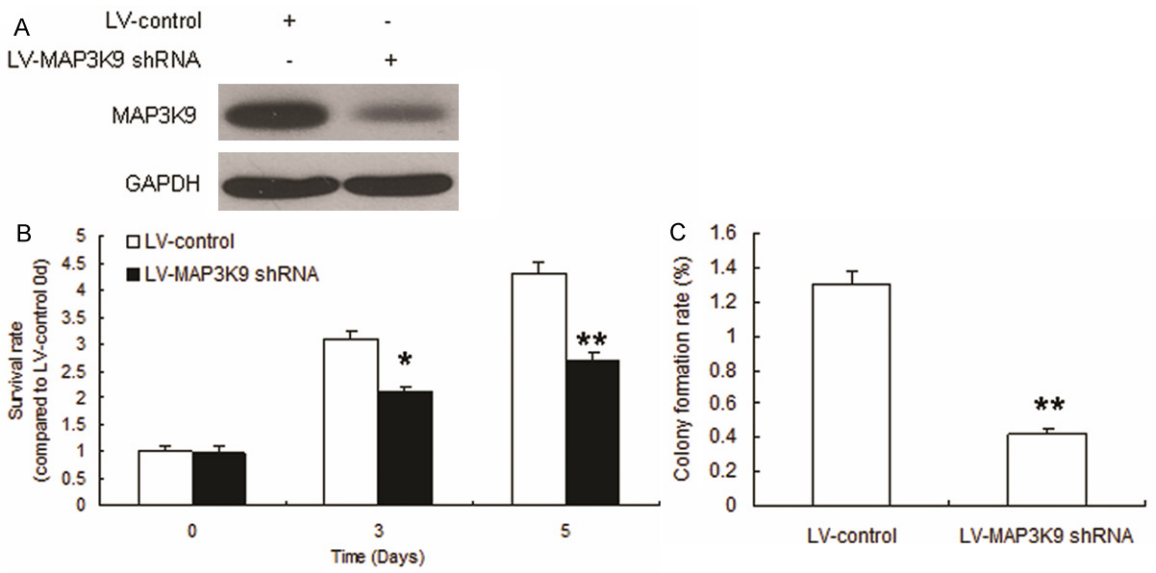

Figure 5. MAP3K9 promotes OS proliferation and shows stem cells properties. A. $CD117^+Stro\text{-}1^+$ cells were infected with LV-MAP3K9 shRNA. Total protein was collected for Western blot. B. Cell proliferation was analyzed by MTT assay. $CD117^+Stro\text{-}1^+$ cells cells were seeded in 96-well plate, added MTT in the day of 3 and 5 and then recorded at the wavelength 570 nm. C. Stem cell sphere formation was performed in $CD117^+Stro\text{-}1^+$ cells with MAP3K9 knocking down. The cells were cultured in medium especially for stem cells and counted the spheres after 2 weeks. Experiments were repeated for at least three times. $^{**}P < 0.01$ compared with scramble group. $^{*}P < 0.05$ compared with scramble group.

mediated MAP3K9 shRNA and MAP3K9 was effectively knocked down (**Figure 5A**). The results of MTT assay showed that cell proliferation was inhibited in cells with MAP3K9 down-regulation (**Figure 5B**). It was also found that stem cell formation ability was suppressed in the MG63 cells with $CD117^+Stro\text{-}1^+$ (**Figure 5C**).

Discussion

Cancer stem cells have been defined as cells within a tumour that possess the capacity to self-renew and to cause the heterogeneous lineages of cancer cells that comprise the tumor [13]. These two definitive biological properties are what make the CSCs the prime candidate for initiation of relapse. Cell surface markers of CSCs can help distinguish, isolate and purify these tumor-initiating cells for further biological investigation. $CD117^+stro\text{-}1^+$ cells comprised a small fraction of the total tumor population in all three samples studied, but represented an increased percentage of the sphere-forming cells. This suggests that $CD117^+stro\text{-}1^+$ could act as a cell surface marker for CSCs in pancreatic cancer. We also investigated the use of this cell surface protein as a candidate marker to further identify the CSC phenotype in OS. The self-renewal ability of $CD117^+stro\text{-}1^+$ cells was tested using spheroid-forming assays in serum-free medium. $CD117^+stro\text{-}1^+$ cells possessed higher clonogenicity than their antigen-negative counterparts. Subsequent *in vivo* tumorigenesis experiments demonstrated that $CD117^+stro\text{-}1^+$ cells possessed higher tumorigenicity than the negative subpopulation. Furthermore, the tumors generated in nude mice displayed the same phenotype as the primary pancreas tissue. Taken together, these results firmly suggest that $CD117^+stro\text{-}1^+$ cells possess the potentials for self-renewal and high tumorigenicity, exhibiting cancer stem-cell-like characteristics in human OS.

Our data provide the first evidence that miR-1247 is able to inhibit CD117 and stro-1 positive tumor sphere-forming and tumor-initiating cancer stem cells in OS, implying that miR-1247 might play a role in the self-renewal of OS stem cells. Similar results were also observed in OS cells, where lentiviral miR-1247 restoration significantly inhibited the clonogenic growth and tumor spheres. We used bioinformatics to search potential target genes and found that MAP3K9 was a target gene of miR-1247. miR-1247 could inhibit cell proliferation, stem cell properties and metastasis. Previous reports show that MAP3K9 is a member of the mixed

lineage family of kinases and is composed of an SH3 domain, Ser/Thr kinase domain, and a Cdc42/Rac interactive binding (CRIB) domain [14, 15]. This kinase is an upstream activator of the JNK and ERK pathways [16]. The role of MAP3K9 in cancer is not well defined; our results showed that interference of MAP3K9 inhibits OS cell proliferation and metastasis.

In summary, we identified miR-1247 to be a tumor suppressor miRNA in OS cancer, and low miR-1247 expression was an unfavorable prognostic factor in patients with OS. miR-1247 partially influences human OS through the regulation of MAP3K9. These results suggest that miR-1247 is a potential target for treating OS cancer and the critical roles of miR-1247 in OS cancer tumorigenesis may aid patient prognosis and diagnosis. Our findings provide basic information to better understand the pathogenesis of OS and its possible therapeutic strategies.

Acknowledgements

The study was supported by the projects of Anhui Province for Excellent Young Talents in Universities (2013SQRL049ZD) and Anhui Provincial Department of Health (KJ2012Z251).

Disclosure of conflict of interest

None.

Address correspondence to: Dr. Qiong Wu or Dr. Yuqing Chen, Departments of Medical Oncology and Respiratory Diseases, The First Affiliated Hospital of Bengbu Medical College, 287 Changhuai Road, Bengbu, Anhui 233000, China. Tel: 86-0552-3175275; E-mail: qiongwu68@yahoo.com.cn (QW); Tel: 86-0552-3175274; E-mail: bbmccyq@126.com (YQC)

References

[1] Wu PK, Chen WM, Chen CF, Lee OK, Haung CK, Chen TH. Primary osteogenic sarcoma with pulmonary metastasis: clinical results and prognostic factors in 91 patients. Jpn J Clin Oncol 2009; 39: 514-22

[2] Jaffe N. Osteosarcoma: review of the past, impact on the future. The American experience. Cancer Treat Res 2009; 152: 239-62.

[3] Meyers PA. Muramyl tripeptide (mifamurtide) for the treatment of osteosarcoma. Expert Rev Anticancer Ther 2009; 9: 1035-49.

[4] Zeng W, Wan R, Zheng Y, Singh SR, Wei Y. Hypoxia, stem cells and bone tumor. Cancer Lett 2011; 313: 129-36.

[5] Tang N, Song WX, Luo J, Haydon RC, He TC. Osteosarcoma development and stem cell differentiation. Clin Orthop Relat Res 2008; 466: 2114-30.

[6] Tian J, Li X, Si M, Liu T, Li J. CD271+ osteosarcoma cells display stem-like properties. PLoS One 2014; 9: e98549.

[7] Adhikari AS, Agarwal N, Wood BM, Porretta C, Ruiz B, Pochampally RR, Iwakuma T. CD117 and Stro-1 identify osteosarcoma tumor-initiating cells associated with metastasis and drug resistance. Cancer Res 2010; 70: 4602-12.

[8] Hayes J, Peruzzi PP, Lawler S. MicroRNAs in cancer: biomarkers, functions and therapy. Trends Mol Med 2014; 20: 460-469.

[9] van Rooij E, Kauppinen S. Development of microRNA therapeutics is coming of age. EMBO Mol Med 2014; 6: 851-64.

[10] Nugent M. MicroRNA function and dysregulation in bone tumors: the evidence to date. Cancer Manag Res 2014; 6: 15-25.

[11] Baglìo SR, Devescovi V, Granchi D, Baldini N. MicroRNA expression profiling of human bone marrow mesenchymal stem cells during osteogenic differentiation reveals Osterix regulation by miR-31. Gene 2013; 527: 321-31.

[12] Novello C, Pazzaglia L, Cingolani C, Conti A, Quattrini I, Manara MC, Tognon M, Picci P, Benassi MS. miRNA expression profile in human osteosarcoma: role of miR-1 and miR-133b in proliferation and cell cycle control. Int J Oncol 2013; 42: 667-75.

[13] Sulzbacher I, Birner P, Toma C, Wick N, Mazal PR. Expression of c-kit in human osteosarcoma and its relevance as a prognostic marker. J Clin Pathol 2007; 60: 804-7.

[14] Slattery ML, Lundgreen A, Wolff RK. MAP kinase genes and colon and rectal cancer. Carcinogenesis 2012; 33: 2398-408.

[15] Stark MS, Woods SL, Gartside MG, Bonazzi VF, Dutton-Regester K, Aoude LG, Chow D, Sereduk C, Niemi NM, Tang N, Ellis JJ, Reid J, Zismann V, Tyagi S, Muzny D,Newsham I, Wu Y, Palmer JM, Pollak T, Youngkin D, Brooks BR, Lanagan C, Schmidt CW, Kobe B, MacKeigan JP, Yin H, Brown KM, Gibbs R, Trent J, Hayward NK. Frequent somatic mutations in MAP3K5 and MAP3K9 in metastatic melanoma identified by exome sequencing. Nat Genet 2011; 44: 165-9.

[16] Thompson NA, Haefliger JA, Senn A, Tawadros T, Magara F, Ledermann B, Nicod P, Waeber G. Islet-brain1/JNK-interacting protein-1 is required for early embryogenesis in mice. J Biol Chem 2001; 276: 27745-8.